Bifurcation, efficiency, and the role of injection in shock acceleration with the Bohm diffusion

M. A. Malkov
Max-Planck-Institut für Kernphysik, D-69029, Heidelberg, Germany;
malkov@boris.mpi-hd.mpg.de

Received _____; accepted _____

ABSTRACT

The efficiency and uniqueness of the diffusive shock acceleration is studied on the basis of the novel kinetic solutions. These solutions obtained earlier (paper I) selfconsistently describe a strong coupling of cosmic rays with the gas flow. They show that the dependence of the acceleration efficiency upon physical parameters is critical in nature. In this paper we investigate a steady acceleration in the parameter space formed by the injection rate ν, the upper cut-off momentum p_1 and the Mach number M while the flow compression R serves as an order parameter. We determine a manifold of all possible solutions in this parameter space.

To elucidate the differences between the present kinetic results and the well known two-fluid predictions we particularly focus on the $\nu \to 0$, $M \to \infty$ limit where the two-fluid model suffers from especially serious closure problems and displays an 'unphysical' behavior. We show that in contrast to the two-fluid model three different solutions occurs also for arbitrarily large M provided that p_1 is sufficiently high. The three solutions appear together only if the injection rate ν lies between two critical values, $\nu_1 < \nu < \nu_2$. For $\nu < \nu_1(M, p_1)$ only the inefficient solution is possible. For $\nu > \nu_2(M, p_1)$ only the efficient solution with a very high cosmic ray production rate occurs. On the basis of the obtained bifurcation surface $R(\nu, p_1)$ we consider the limit $p_1 \to \infty$, $\nu \to 0$ which completely uncovers the long debating anomalies of the two-fluid model.

The constructed steady state manifold that, at least partially is an attractor of a time dependent system, allows us to speculate on the nonstationary acceleration.

Subject headings: acceleration of particles, cosmic rays, diffusion, hydrodynamics, shock waves, supernova remnants

1. Introduction

The question, how efficient the diffusive shock acceleration may be, arose naturally when the first test particle calculations of this process became available (Krimsky 1977; Axford, Leer & Skadron 1977; Bell 1978; Blandford & Ostriker 1978; see Drury 1983; Blandford & Eichler 1987 and Jones & Ellison 1991 for a review). This is because the backreaction of accelerated particles (cosmic rays (CRs) in the astrophysical context) on the shock structure is very strong and leads normally to a significant increase of the compression ratio. Such an accelerating shock should therefore be thought of as a strongly nonlinear dynamical system with a pronounced selforganization. Neither the particle spectrum nor the hydrodynamic flow structure can be calculated independently. Furthermore, since the diffusion length of particles increases with momentum, particles with higher momenta sample longer parts of the shock transition. This makes any kind of moment description very difficult. However, the first essentially nonlinear calculations of this acceleration process were performed within the hydrodynamic approach.

1.1. Success and limitations of the two-fluid model

The above arguments suggest that the problem is kinetic in nature, which makes the usage of any fluid theory for describing the acceleration process questionable. At the same time quite a deep insight can be gained from simple moment equations. The two-fluid model (TFM) introduced by Axford Leer & Skadron (1977) and Drury & Völk (1981) (DV, hereafter) treats the thermal and CR populations as separate fluids coupled only through the hydrodynamic equations. The main effect of this coupling is a deceleration of the inflowing gas in front of the shock by the pressure gradient of counterstreaming CRs accelerated at the shock and, as a result, an enhancement of the total shock compression, the multiplicity of solutions and a much higher acceleration efficiency. Unfortunately, the underlying particle distribution implies the pressure divergence and is underdetermined in some other ways (see *e.g.,* Drury 1983; Achterberg, Blandford & Periwal 1984; Kang & Jones 1990, and below).

1.2. Renormalization of the two-fluid model

A renormalization procedure to overcome the above ultraviolet divergence has been suggested recently by Malkov & Völk (1996) (MV96, hereafter). This theory produces basically the same two-fluid hydrodynamics except the renormalized CR specific heat ratio Γ instead of the usual γ_c which results from the losses. Under the assumption $\gamma_c = 5/3$ upstream (which automatically implies that far upstream $\Gamma = 5/3$ as well, for the case of reacceleration considered in MV96), $\gamma_c = 4/3$ downstream, and in the limit $p_1 \to \infty$, the

renormalized two-fluid model (RTFM) produces a solution qualitatively similar to that of the unrenormalized theory. In the case of $\gamma_c = 4/3$ upstream, when also Γ decreases $\Gamma < \gamma_c$, the results change dramatically. Namely, the shock compression r becomes much larger than the usual unrenormalized result $r = 7$ (for strong shocks). What happens is a very fast increase of the losses with decrease of γ_c which rises the compression that even tends to infinity (for infinitely large Mach numbers when, in addition, one takes the maximum possible spectral slope $q = 3r/(r-1)$ at the upper cut-off). This regime was not (and could not be) explored in MV96 since such a high compression shock requires a detailed information about γ_c, Γ, and $\bar{\kappa}$, the spectrum averaged CR-diffusivity across the shock transition. This would practically be equivalent to the full kinetic solution. To obtain such a solution was one of the main objectives of a companion paper (Malkov 1997a, paper I). Further motivations of the present paper will be outlined in the next subsection.

To conclude this subsection we note that the assumption $\gamma_c \approx 4/3$ upstream is precisely what the kinetic solution obtained in paper I suggests for the case of injection in contrast to the case of reacceleration, $\gamma_c = 5/3$ considered in MV96. Moreover, γ_c is smaller upstream than downstream, again opposite to the reacceleration case. Finally, the RTFM results in the injection case are unacceptably sensitive to the values of γ_c and Γ that are not known to the required extent when the kinetic solution is not available. This makes the moment approach especially restrictive for describing namely the injection triggered acceleration process. As in paper I we concentrate here on this, certainly more interesting and at the same time more difficult case.

1.3. 'Pathological' limits of the TFM

There exists another difficulty of the TFM that has already been criticized in the literature (*e.g.,* Jones & Ellison 1991). Namely, the shock modification in a steady state occurs while particles are constantly injected at some rate, are then accelerated, and disappear eventually through the upper cut-off or downstream. Once the injection is somehow eliminated, the CR-dominated (or efficient) steady-state solution cannot be justified physically, and the ordinary gas shock remains the only solution possible. The TFM, however, still produces a CR-dominated shock that even becomes completely smooth beyond a certain Mach number, $M > M_1$. In fact, it represents a fast-mode shock in a two-fluid hydrodynamics associated with the tenuous high pressure CR-fluid (Ptuskin, 1981). Since the number density of the CRs n_c is irrelevant in the TFM, solutions that have a finite CR pressure ($P_c > 0$) are formally permitted without any injection ($n_c = 0$). Moreover, for an arbitrarily small nonzero injection rate there exists a critical Mach number $M_2 < \infty$ above which this efficient solution is the only one the TFM can offer.

Clearly, it is difficult to judge the acceleration efficiency because the injection rate is, as a rule, very small and the two-fluid system, on the other hand, does not behave adequately

when injection vanishes. The question, however, is whether the consideration of this limit within the TFM is admissible. The answer is definitive not. Indeed, a fully kinetic steady state solution obtained in paper I revealed the following nonlinear response of the system to a weak injection of thermal particles. First of all, this response depends not so much on the injection itself but rather on the parameter $\Lambda_1 = \nu/\delta \equiv \nu p_1/p_0$, where ν and p_0 are the injection rate and injection momentum, respectively, and $\delta \ll 1$. Furthermore, the effect of shock modification completely disappears as $\Lambda_1 \to 0$ (it becomes practically insignificant in an abrupt manner already at $\nu/\sqrt{\delta} \lesssim 1$). Only in the other extreme, $\Lambda_1 \to \infty$ (more precisely, when $\Lambda_1 \gg M^{3/4}$, see also subsection 4.1) a *unique* solution that is indeed injection insensitive appears which is quite in the spirit of the TFM. Quantitatively, this solution can be very different from the respective TFM solution but for a different reason which is related to the subshock smoothing. The TFM is of course incapable of describing the dependence of its solution on Λ_1 since it implies $p_1 = \infty$, i.e. $\Lambda_1 = \infty$ already on the derivation level; even if ν is set to zero afterwards the physically correct behavior of the solution with vanishing injection cannot be recovered since Λ_1 remains infinite. Therefore it is useless to expect from the TFM a correct behavior at $\nu \to 0$ and to criticize this model for the lack of it. This is beyond its validity range.

The most dramatic consequence of this ($p_1 \to \infty$) degeneracy is the subshock smoothing ($r_\mathrm{s} \equiv 1$). The solution becomes enormously different from the kinetic solution that does not pass through the point $r_\mathrm{s} = 1$ just because of this fact. Why this is so, has been explained in paper I and we shall look at this problem from a different perspective in subsection 4.1.

Perhaps the most direct explanation why the kinetic solution differs so strongly from its hydrodynamic counterpart is the singular character of the underlying perturbation problem in the small parameter $\delta \equiv p_0/p_1 \ll 1$. No matter how small it is, the efficient kinetic solution with $\delta = 0$ (and, hence, the TFM solution) is fundamentally different from that with $\delta > 0$ (see paper I).

The parameters that the TFM usually operates on are the Mach number M and the injection rate ν (or the seed particle pressure in the case of reacceleration). As we argued, this is not enough to describe consistently what is going on in the steady nonlinear shock acceleration. The RTFM introduces an additional parameter needed, p_1, and accounts of the losses at $p = p_1$ but then it lets $p_1 \to \infty$, ν fixed. That means $\Lambda_1 \equiv \nu/\delta \to \infty$, and therefore the results are again insensitive to ν when $\nu \to 0$ since the critical information about Λ_1 is lost, exactly as in the TFM. We emphasize that it is the parameter Λ_1 that regulates primarily the budget of energetic particles at a shock, not ν alone. That is why, for example, the subshock completely vanishes in the TFM as well as in the RTFM beyond a certain $M = M_1$ even for $\nu \to 0$; the more important parameter Λ_1 remains infinite which effectively corresponds to the situation with a very strong injection.

If we allow for time dependence on the kinetic level of description and assume a slower than in the Bohm limit momentum dependence of the CR diffusion coefficient, completely

smooth TFM stationary solutions will exist even with zero injection and with no seed particles upstream. This phenomenon has been explained by Drury (1983)– the high energy particles may be considered as those injected in the past and being then continuously accelerated at the shock. Unfortunately the smooth TFM solutions can tell us very little about a steady acceleration of CRs out of the thermal upstream plasma – if there are no preexisting CRs, there are no such solutions.

Since these TFM solutions are essentially time dependent on the kinetic level (see *e.g.,* Falle & Giddings 1987, Kang & Jones 1990 and Drury, Völk & Berezhko 1995 for relevant discussions), we may infer that once a natural cut-off $p_1 < \infty$ exists and is reached, this acceleration regime will be disrupted. Indeed, these solutions correspond to the acceleration of CRs injected in the past whose number density virtually decreases (although being irrelevant in the TFM which in fact admits these pseudo-steady solutions) while the CR pressure remains approximately constant, being determined simply by the ram pressure of the inflowing gas. When particles start to leak through the upper cut-off the CR pressure decreases as well and the system relaxes to the ordinary gas shock which is the only steady state solution without injection. In general, the above TFM quasi-stationary acceleration scenario implies a rather low production of CRs (in terms of their number, not the energy density) because it operates only on initially injected particles and suppress further injection as soon as this solution is set up. Much more productive would be solutions that allow for permanent losses. This would mean, in fact, the propagation of high-energy CRs into the shock surroundings which decouples them from the gas flow with their replenishment due to the permanent injection at the subshock. But these solutions are essentially kinetic and, as we emphasized, fairly different from the TFM solutions.

As it was demonstrated in paper I, given the injection rate three different solutions are possible for sufficiently high M and p_1, Figure 1. However, only the most efficient solution with the highest compression ratio has been considered in detail. Accordingly, only a first critical injection, i.e. the injection rate $\nu = \nu_1$ above which this solution exists along with the two other solutions has been calculated. The calculation of a second critical injection that requires an inspection of the two remaining solutions and above which the efficient solution is the only possible, is one of the subjects of the present paper. We consider the entire manifold of stationary solutions and in this context the three above-mentioned solutions are simply its subsets.

In the next section we briefly review the physical formulation of the problem and discuss our strategy of a unified description of all the three solutions. In Sec.3 we obtain both the efficient and inefficient solutions from the integral equation derived in paper I and consider their matching in an intermediate range. In Sec.4 we describe the solution space as a whole and calculate the critical injections. We conclude this section with implications of its results for the TFM . Further, in Sec.5 we speculate upon possible scenarios of time dependent acceleration on the basis of the emerged bifurcation picture. Sec. 6 discusses the results and some of their most evident consequences for calculations of the acceleration

efficiency in real astrophysical objects.

2. Kinetic solution

The standard formulation of the problem of diffusive shock acceleration includes the diffusion-convection equation for the high energy particles constrained by conservation of the fluxes of mass and momentum (see *e.g.,* Drury 1983; Blandford & Eichler 1987). The physical situation that we shall consider throughout this paper is described in paper I and we quote only the key elements below.

2.1. Overview of the physical formulation

We assume that a strong CR-modified shock propagates in the positive x-direction and in the shock frame of reference the steady state velocity profile of the gas is specified as follows: $U(x) = -u(x)$ for $x \geq 0$, $u(0+) = u_0$; $u(\infty) = u_1$. The equation that describes the isotropic part of particle distribution $g(x, p)$ at sufficiently high momenta is the diffusion-convection equation (Parker 1965; Gleeson & Axford 1967) which in the region $x \geq 0$ takes the form

$$\frac{\partial}{\partial x}\left(ug + \kappa(p)\frac{\partial g}{\partial x}\right) = \frac{1}{3}\frac{du}{dx}p\frac{\partial g}{\partial p} \tag{1}$$

Here κ denotes the particle diffusion coefficient that is assumed to be $\kappa(p) = \kappa_0 p/p_0 = \kappa_1 p/p_1$, where p_0 and p_1 are the injection and cut-off momenta, respectively and the number density of the CRs is normalized to $4\pi g dp/p$. In the downstream region ($x < 0$) we choose, as usual, a spatially homogeneous solution given by $U(x) \equiv -u_2 = const$ and $g(x, p) \equiv g_0(p)$. Thus u_2 is the (constant) downstream speed. Eq.(1) governs the process of stationary acceleration of the CRs that are drawn (injected) from the thermal plasma at $p \sim p_0$ and leave the system at $p = p_1 \gg p_0$. Since the pressure of accelerated particles directly influences the flow profile $u(x)$ in the shock precursor, eq.(1) should be complemented by the conditions of the mass and momentum conservation

$$\rho u = \rho_1 u_1, \tag{2}$$

$$P_{\rm c} + \rho u^2 = \rho_1 u_1^2 \tag{3}$$

Here $\rho(x)$ is the mass density, $\rho_1 = \rho(\infty)$, $P_{\rm c}$ is the CR pressure

$$P_{\rm c}(x) = \frac{4\pi}{3}mc^2\int_{p_0}^{p_1}\frac{pdp}{\sqrt{p^2+1}}g(p, x) \tag{4}$$

and no seed particles are present, i.e. $P_{\rm c}(\infty) = 0$. The particle momentum p is normalized to mc. Eq.(3) is written in the region $x > 0$ where we have neglected the contribution

of the adiabatically compressed cold gas confining our consideration to sufficiently strong shocks with $M^2 \equiv \rho_1 u_1^2/\gamma P_{\rm g1} \gg (u_1/u_0)^\gamma$, where γ is the specific heat ratio of the plasma (see paper I for a detailed discussion of this approximation).

The subshock strength can be determined from the ordinary Rankine-Hugoniot condition for the gas

$$r_{\rm s} \equiv \frac{u_0}{u_2} = \frac{\gamma+1}{\gamma-1+2M^{-2}R^{\gamma+1}} \tag{5}$$

where $R = u_1/u_0$.

2.2. Invariant form of the solution

It is quite clear that the formal solution to eq.(1) can be regularly found as a series in parameter $(u_1 - u_0)/u_0$ if the latter is small. Fortunately (see paper I and Malkov 1997b) also in the case of a very strong modification ($u_1 \gg u_0$) the structure of the solution does not change significantly, provided that it is written in appropriate variables. The key variable here is simply the flow potential

$$\Psi = \int_0^x u dx \tag{6}$$

and the approximate solution in both cases can be represented as

$$g = g_0(p) \exp\left\{-\frac{1+\beta}{\kappa}\Psi\right\} \tag{7}$$

If the solution is efficient ($u_1 \gg u_0$), β is given by the following relation

$$\beta \equiv -\frac{1}{3}\frac{\partial \ln g_0}{\partial \ln p} \tag{8}$$

In the case of inefficient solution ($u_1 \approx u_0$) the β-term in eq.(7) should be omitted altogether. In fact, there is no much difference between these two cases as far as the formal representation of the solution is concerned; as it was shown in paper I, for efficient solutions $\beta \approx 1/6$ over a broad momentum range. On the other hand the explicit dependence of these solutions on p and x can be vastly different in these two cases since both the flow potential and the downstream spectrum may differ dramatically. It is important to emphasize that it is this latter circumstance that constitutes the nonlinearity of the acceleration process, not the difference between the representations of the efficient and inefficient solutions by the formula (7) which is reflected in the β term. The calculations in paper I show that this β term results in a numerical factor $\theta \approx 1.09$ in the expression for the shock compression ratio instead of $\theta = 1$, that one would get without β term in the solution (7), i.e. taking it in the form of inefficient solution. Thus eq.(7) may be regarded as an invariant form of

the approximate kinetic solution. It creates a perspective of universal description of fairly different acceleration regimes. For this purpose we extend the technique developed in paper I for describing the efficient and intermediate solutions to the case of inefficient solution. Acting within the above-mentioned 'ten percent' accuracy ($\theta = 1.09 \approx 1$), we will handle the θ-factor somewhat loosely, putting $\theta = 1$ in final results when we apply them to the inefficient part of the solution without a more accurate matching. The price that we pay for the universality of description of all the three branches is not high, if one realizes that the global bifurcation properties of the system under question are not really known even qualitatively.

3. Unified description of the acceleration process

The basis of a universal treatment of acceleration solutions is established in paper I and its critical step is the derivation of an integral equation for a normalized spectral function

$$J(p) = \frac{\bar{V}(p)}{\bar{V}(p_0)} \tag{9}$$

where $\bar{V}$ is the spectral function introduced by the following relation

$$\bar{V}(p) = \int_{0-}^{\infty} e^{-s(p)\Psi} du(\Psi) \tag{10}$$

with

$$s(p) = \frac{1}{\kappa(p)\bar{V}(p)} \left[u_2 + \bar{V}(p) + \frac{1}{3} \frac{\partial \bar{V}}{\partial \ln p} \right] \tag{11}$$

The explicit dependence of the variable s on $\bar{V}$ is not very critical here since $\bar{V}$ effectively cancels out in eq.(11) and eq.(10) should be regarded logically as an integral transform $u(\Psi) \mapsto \bar{V}(p)$ rather than an equation for $\bar{V}(p)$ given $u(\Psi)$. An independent integral equation for $\bar{V}(p)$ (or J) was, in turn, derived from the Bernoulli's integral (3). Using a number of approximations discussed in paper I, this equation can be written down as follows

$$J(\tau) = \frac{\zeta}{\varepsilon} \int_{\varepsilon}^{\varepsilon^{-1}} \frac{d\tau'}{\tau' + \tau} \frac{1}{\tau' J(\tau')} \exp\left[\frac{3}{\theta(r_{\rm s} - 1)} \int_{\varepsilon}^{\tau'} \frac{d\tau''}{\tau'' J(\tau'')} \right] + 1. \tag{12}$$

We have used the notations

$$\zeta = \nu R \exp\left[-\frac{3}{\theta(r_{\rm s} - 1)} \int_{\varepsilon}^{1/\varepsilon} \frac{d\tau''}{\tau'' J(\tau'')} \right] \tag{13}$$

$$\tau = \frac{\kappa_0 s}{\varepsilon} \left(1 - \frac{1}{r_{\rm s}} \right); \quad \varepsilon^2 = \left(1 - \frac{1}{r_{\rm s}} \right) \frac{p_0}{p_1} \theta \ll 1; \tag{14}$$

We use here ν as the injection rate that differs from the injection rate η used in paper I and is specified as follows

$$\nu \equiv p_0\eta \simeq \frac{p_0 r_{\rm s}}{r_{\rm s}-1}\frac{mn_{\rm c}c^2}{\rho_1 u_1^2} \tag{15}$$

where

$$n_{\rm c} = 4\pi\int_{p_0}^{\infty} g_0(p)dp/p \tag{16}$$

In order to close the system formed by eqs.(5) and (12) we need another equation to relate the three variables $(\nu, R, r_{\rm s})$ among whose only one, say ν we consider as given. As an intermediate step we relate the precursor compression R and the spectral function J by inverting eq.(10):

$$\frac{du}{d\Psi} = \frac{1}{2\pi i}\int_{-i\infty}^{i\infty} e^{s\Psi}\bar{V}(s)ds + \Delta u\delta(\Psi) \tag{17}$$

where δ is a delta function corresponding to the jump of u at the subshock. Integrating then eq.(17) over Ψ between $\Psi = 0+$ and ∞ we get

$$u_1 - u_0 = \frac{\Delta u}{2\pi i}\int_{-1/\varepsilon}^{-\varepsilon}\frac{d\tau}{\tau}\left[J(\tau+i0) - J(\tau-i0)\right] \tag{18}$$

We have put $\bar{V}(p_0) \approx \Delta u$ (see paper I for details concerning this approximation). The integral around the cut $(-1/\varepsilon, -\varepsilon)$ may be evaluated with the help of eq.(12) and the last equation rewrites

$$\frac{R-1}{1-r_{\rm s}^{-1}} = \frac{\zeta}{\varepsilon}U \tag{19}$$

where

$$U = \int_{\varepsilon}^{1/\varepsilon}\frac{d\tau}{\tau^2 J(\tau)}e^{\Omega\phi(\tau)} \tag{20}$$

with

$$\Omega = \frac{3}{\theta(r_{\rm s}-1)} \quad \text{and} \quad \phi(\tau) = \int_{\varepsilon}^{\tau}\frac{d\tau'}{\tau' J(\tau')} \tag{21}$$

In general, the system formed by eqs.(5), (12), and (19) may have multiple solutions. On the other hand for sufficiently small injection rates ν there must always be a solution to eq.(12) that corresponds to the test particle acceleration regime in which $J \to 1$ as $\nu \to 0$. This solution can be written down in terms of a Neuman series in ν or ζ as follows

$$J = 1 + \frac{\zeta}{\varepsilon^2}\ln\frac{\varepsilon^{-1}+\tau}{\varepsilon+\tau} + \mathcal{O}(\zeta^2) \tag{22}$$

where we have put $\theta = 1$ (see the preceding section) and $r_{\rm s} = 4$ for simplicity. Solution (22) is essentially perturbative and cannot describe two remaining solutions of eq.(12) that appear beyond some $\nu = \nu_1 > 0$. As we shall see all the three solutions may be conveniently described by the single valued function $\nu = \nu(R)$ in the (R, ν) plane (Figure 1). We term

the solution with $R > R_1$ efficient, and that with $R_2 < R < R_1$ – intermediate. It merges with the inefficient solution at the point $\nu = \nu_2, R = R_2$. For a fixed $\nu \in (\nu_1, \nu_2)$ all the three solutions have different values of R and hence different subshock compression ratio r_s.

For the further bifurcation analysis the following relation appears to be useful. It may be derived from eq.(12) by multiplying both sides by $(1/\tau^2 J)\exp(\Omega\phi)$ and integrating then the result between ε and ε^{-1}:

$$\frac{\zeta}{2\varepsilon}U^2 + (1-\Omega)U + \varepsilon e^{\Omega\phi_0} - \frac{1}{\varepsilon} = 0 \tag{23}$$

where

$$\phi_0 \equiv \phi(\epsilon^{-1})$$

Summarizing this subsection we note that eqs.(5), (12), and (19) form a closed system for describing all the three branches of the solution.

3.1. Branches 2 and 3

As we mentioned the branches 2 and 3 of the function $R(\nu)$ in Figure 1 were studied in paper I with the emphasis on the branch 3, that corresponds to the efficient solution. In this approximation $J \gg 1$ and hence one may neglect the second term on the right hand side (r.h.s.) of eq.(12) as well as the term in the exponent since $\zeta \gg \varepsilon$. After the formal solution of the resulting equation for J is obtained, eq.(13) for ζ serves as a nonlinear 'dispersion relation' for this system. There is a pair of solutions in the region $\nu > \nu_1$ and there are no solutions if $\nu < \nu_1$ within the approximation $\zeta \gg \varepsilon$. Note that the inefficient solution (branch one, $\zeta \ll \varepsilon$) still exists and remains the only possible for $\nu < \nu_1$. The above approximation becomes better and better with increasing $\nu > \nu_1$ for the branch 3 (ζ grows with ν) and it becomes worse for the branch 2, since in the latter case ζ decreases and the neglected terms become more and more important. We obtain here the part 2-3 of the bifurcation curve $R(\nu)$ in Figure 1 direct from eq.(23) rather than from the explicit solution of eq.(12) as it was done in paper I. The former procedure is more convenient for matching with the rest of this curve. First, neglecting the second and the third terms eq.(23) simplifies to

$$U \simeq \sqrt{\frac{2}{\zeta}} \tag{24}$$

The last approximation, being strictly valid for the branch 3, is also good on some part of the branch 2 provided that (see eqs.(13,23))

$$\frac{\sqrt{\zeta}}{\varepsilon} \gtrsim |1-\Omega| \tag{25}$$

$$\sqrt{\zeta} \gtrsim \frac{1}{\ln 1/\varepsilon} \tag{26}$$

Inequality (26) may be obtained estimating the integral in eq.(13) as $\sqrt{2/\zeta}$ (paper I). These conditions are, generally speaking, opposite to the validity condition of the low ζ expansion (22) (branch 1) that is

$$\sqrt{\zeta} < \varepsilon \tag{27}$$

This makes the analytic description of the intermediate branch 2 (Figure 1), where $\sqrt{\zeta}$ may approach ε, more difficult as it was explained earlier. Fortunately, the factor $|1-\Omega|$ in eq.(25) is rather small numerically, unless $r_s \approx 1$, and there exists an intersection between the half-intervals (25) and (27). The smallness of $|1-\Omega|$ is ensured by the facts that $\theta - 1$ is numerically small and r_s is close to 4 on the branch 2 since R is appreciably smaller there than on the branch 3 for the same M and ν. The inequality (26) is formally much more restrictive regarding the matching with the branch 1. Nevertheless, as we shall see in the next subsection, a quite accurate matching is still possible because the branch 1 can in fact be extended to the region (26). Besides that the third term in eq.(23), whose neglecting requires the constraint (26), will not significantly exceed, in fact, the last term even for $R \ll R_1$ (see eq.(32) below). Coming back to eq.(19) for the flow compression R we obtain

$$R - 1 = \frac{3\sqrt{2\zeta}}{4\varepsilon}\left(1 - \frac{R^{8/3}}{M^2}\right) \tag{28}$$

We have used eq.(5) with $\gamma = 5/3$ and eq.(24). Now we are able to obtain the 2-3 piece of the curve $\nu = \nu(R)$. On the branch 3 and partly on the branch 2 not far from the critical point (ν_1, R_1) we may replace the integral in eq.(13) by $\sqrt{2/\zeta}$. Eq.(13) can thus be transformed to the required form

$$\nu(R, M) = \frac{\zeta}{R}\exp\left(\frac{1}{\theta}\sqrt{\frac{2}{\zeta}}\frac{1 + 3R^{8/3}M^{-2}}{1 - R^{8/3}M^{-2}}\right) \tag{29}$$

where the function $\zeta(R, M)$ should be taken from eq.(28). The function ν is plotted against R for $M = \infty$ and $\delta \equiv p_0/p_1 = 10^{-4}$ in Figure 2 with the dashed line. As we mentioned this solution fails to work for R sufficiently smaller than R_1 (Figure 1) and should be replaced by a different solution that must be valid down to $R = 1, \nu = 0$. The overlapping region to match both asymptotic solutions is presumably within the interval $R_2 < R < R_1$. For this purpose we obtain in the next subsection an approximate solution that describes the branch 1 reasonably well, in particular it yields a qualitatively correct behavior for $\nu \to 0$, is also valid for the branch 2 and may thus be matched with the solution (29).

3.2. Branches 1 and 2

The key step here is to rewrite eq.(12) as follows

$$J(\phi) = \frac{\zeta}{\varepsilon}\int_0^{\phi_0} \frac{d\phi'}{\tau(\phi') + \tau(\phi)} e^{\Omega\phi'} + 1 \tag{30}$$

where the function $\tau(\phi)$ is defined by eq.(21). Our nearest goal is to work out a usable approximation to the solution of this equation that is good for the region of sufficiently small $R < R_1$. As we have seen in the previous subsection, the branch 3 is characterized by the condition $\Omega\phi_0 \sim 1$ for $R \sim R_1$ and $\Omega\phi_0 \ll 1$ for $R \gg R_1$, which facilitates the study of efficient solution far from the critical point $R = R_1$. Therefore it is natural to use the approximation $\Omega\phi_0 \gg 1$ for $R < R_1$ and to examine the possibility of matching the obtained asymptotic result with the solution (29). In this approximation ($\Omega\phi_0 \gg 1$) the integral in eq.(30) is dominated by its upper limit and we may write it as

$$J(\tau) = \frac{\zeta}{\Omega}\frac{e^{\Omega\phi_0}}{1+\varepsilon\tau} + 1 \tag{31}$$

We will continue the discussion of the accuracy of this approximation for moderate values of $\Omega\phi_0$ in the next section arguing in terms of a very good matching of this solution at $\Omega\phi_0 \sim 1$ with the solution given in the preceding subsection for the 2-3 piece of the curve $\nu(R)$. Substituting now the asymptotic result (31) in eq.(21) we get

$$\phi_0 = \frac{\xi/\Omega}{\xi/\Omega+1}\ln\frac{\xi/\Omega+2}{\xi/\Omega+1} + \frac{2}{\xi/\Omega+1}\ln\frac{1}{\varepsilon} \tag{32}$$

where

$$\xi = \nu R \tag{33}$$

Next, since the flow compression R is not very large for 1-2 branches we can simplify the algebra by using the approximation of infinite Mach number for these branches, i.e we put $r_s = 4$ in eq.(23). This is a good approximation for $R \ll M^{3/4}$. Neglecting also $\theta - 1 \approx 0.1$ compared to $R - 1 \gtrsim 1$, in eq.(23), eqs.(13), (19) and (23) yield

$$(R-1)^2 = \frac{9}{8}\xi\left(\frac{1}{\varepsilon^2}e^{-\Omega\phi_0} - 1\right) \tag{34}$$

The last approximation is formally inaccurate for $R - 1 \lesssim \theta - 1$ as the inspection of eq.(23) may show. On the other hand the qualitative behavior of $\nu(R)$ remains unchanged in this region and is essentially $\nu \sim R - 1$. As we mentioned earlier the value $\theta \approx 1.09$ was calculated in paper I for the efficient (intermediate) solution whereas for the inefficient solution in the region $R - 1 \ll 1$ the value $\theta = 1$ is, in fact, a better choice. In this case eq.(34) is virtually also valid for small $R - 1$ provided that $r_s \approx 4$, which is definitely the case for such a small R. Substituting ϕ_0 from eq.(32) and taking the relation $\Omega \approx 1/\theta$ into account we finally obtain

$$(R-1)^2 = \frac{9}{8}\xi\left[\left(\frac{1+\theta\xi}{2+\theta\xi}\right)^{\frac{\xi}{1+\theta\xi}}\varepsilon^{2\frac{1/\theta-1-\theta\xi}{1+\theta\xi}} - 1\right] \tag{35}$$

Together with the relation (33) this equation determines the 1-2 part of the curve $\nu = \nu(R)$. It is plotted in Figure 2 with the solid line. The both solutions may be matched smoothly by the construction of an appropriate intermediate expansion. It is in fact not needed for our purposes since the deviation of these two solutions is numerically insignificant in an extended region between the intersection points.

4. The overall picture of stationary acceleration

In the preceding section we have demonstrated that the method of integral equation developed in paper I allows one to describe the process of steady shock acceleration on a universal basis, which gives to the notions of efficient and inefficient acceleration a concrete mathematical content in the form of a relevant bifurcation analysis. Although different asymptotic approaches for describing efficient and inefficient regimes are applied in the present study, the both solutions match in the region of the intermediate acceleration regime very well. This is in fact an overlapping region for the two solutions in the sense of the obtained asymptotic results. Generally, the integral equation (12) describes all the three regimes on the same basis so that the matching procedure can be improved and a uniformly valid asymptotic expansion can be constructed. However the achieved accuracy is sufficient for our purposes.

In fact we are already in a position to describe the stationary solution space in terms of system parameters and dependent variables that characterize the acceleration process. In principle, our parameter space is two-dimensional and contains the Mach number M and the cut-off momentum p_1 (we will use the parameter $p_1/p_0 \equiv \delta^{-1} \gg 1$). It should be reminded that our consideration is restricted to the region $M \gg R^{5/6}$, $p_1 \gg 1$ (Sec.2). A convenient dependent variable is the flow compression R that obviously signifies the efficiency of acceleration. In the present study, however, we add to this parameter space also the injection rate ν, since this latter, even though being in principle calculable, may vary depending on the model of the subshock dissipation used (see the corresponding discussion in Appendix A of paper I). Furthermore, as we have seen, the solution may be conveniently represented in the form of a single valued function $\nu(R)$ that is shown in Figure 2. Thus we perform our bifurcation analysis here in three dimensional parameter space. In a future work we will reduce the parameter space to its natural dimensionality (two) by specifying the injection rate given the subshock conditions.

In fact the character of bifurcations may be seen from the surface plots $\nu = \nu(R, M)$ at fixed p_1 and $\nu = \nu(R, p_1)$ at fixed M, respectively. These surfaces are shown in Figure 3a,b. One sees that the multiplicity of the solution $R = R(\nu)$ is always present for sufficiently large values of M and p_1. We have not plotted, however, the region of lower Mach numbers in Figure 3a where the solution indeed becomes unique for all ν. The approximation $M \to \infty$ adopted for describing 1-2 branches is inaccurate there and the usage of eq.(23) is required for plotting the surface $\nu(R, M)$ instead of a simplified version of it given by eq.(24). This is clearly indicated by a less accurate matching of the 1-2 and 2-3 asymptotic solutions for smaller M in Figure 3a. The tendency to the uniqueness for lower M is quite obvious already from this figure. A more accurate investigation of this region can be conveniently done by a numerical solution of eq.(12), or better, of a more general equation in paper I which we leave for a separate study.

As it is seen from Figure 3a, the effect of the finite Mach number M results in the fast

increase of $\nu(R, M)$ in the region $R \lesssim M^{3/4}$, see also Figure 4. Therefore, for sufficiently large $\nu = const$ where $M^{3/4} < \nu/\delta$, R scales as $R \sim M^{3/4}$. In the opposite case, $M^{3/4} > \nu/\delta$ the compression ratio, represented as a function of M saturates at the level $R \sim \nu/\delta$. In this regime the behavior of the solution is close to that for $M = \infty$.

4.1. Critical injections. The TFM paradox revisited

The next issue we address here is the calculation of critical injections ν_1 and ν_2. From eqs.(28) and (29), restricting ourselves for simplicity to the case $M \to \infty$ we calculate[1]

$$\nu_1 = 2e\sqrt{\frac{\delta}{3\theta}}; \quad R_1 = \theta^{-3/2}\sqrt{\frac{3}{\delta}} \tag{36}$$

To calculate ν_2 we simplify eq.(35) as follows. First, as discussed in Sec.2.2 we may set $\theta = 1$. We also assume $\xi \ll 1$ but $\delta^{-\xi} \gg 1$. Then, from eq.(34) we have $(R-1)^2 = \frac{9}{8}\xi\delta^{-\xi}$. Substituting $\xi = \nu R$ for the second critical injection ν_2 and for R_2 we find the following results that we write with a 'logarithmic accuracy'

$$\nu_2 = \frac{2\sqrt{2}}{3}\frac{\sqrt{\ln\ln\frac{1}{\delta}}}{\ln\frac{1}{\delta}}; \quad R_2 = \frac{3}{2\sqrt{2}}\sqrt{\ln\ln\frac{1}{\delta}} \tag{37}$$

Clearly, the nonlinearity of the acceleration process will be important when the CR pressure in front of the shock is comparable with the ram pressure. Therefore, an estimate for ν_2 can be obtained directly from the condition $P_c \simeq \rho_1 u_1^2$. On putting $g_0 \simeq p_0/p$, ($r_s = 4$) into P_c and using the relativistic form of the partial pressure for all p in eq.(4), we get $\nu_2 \simeq 1/\ln(1/\delta)$. A similar approach to estimating the backreaction of injected and subsequently accelerated particles onto the gas flow has been also applied by previous authors (see *e.g.,* Drury, Markiewicz & Völk 1989). The both critical injections (eqs.(36, 37)) are plotted versus δ in Figure 5. One sees from Figs.1 and 5 that the limit $\nu \to 0$ automatically means $R \to 1$ (ordinary gas shock) for all $\delta > 0$. Since ν_2 vanishes with δ much slower than ν_1 there is always a significant gap between these two critical injections, i.e. an extended region of multiple solutions even for very small values of δ.

It is interesting to trace the deformation of the bifurcation curve $\nu(R)$ under the transition to the two-fluid limit. Strictly speaking there is no kinetic prototype for the smooth two-fluid efficient solution ($r_s \equiv 1$) as it was argued earlier. At the same time this is not linked directly with the fact that R fails to tend to unity as $\nu \to 0$ in the TFM

[1]The critical injection ν_1 obtained here without an explicit usage of the solution to eq.(12) differs from the correspondent result (eq.(70)) in paper I by a numerical factor ~ 1. This difference was explained in detail in paper I (see eq.(57) and the text below it).

and we explain this last anomaly of this model first and shall return to the issue of the subshock smoothing later. To simplify the algebra we restrict our consideration to the case $M = \infty$ that is quite representative in this regard. For instance, one gets $R = 7$ from the TFM in this case, also for $\nu = 0$. Let us perform the transition $\delta \to 0+$ (fluid limit) in the kinetic description. According to eqs.(36, 37) we have $\nu_2 \to \nu_1 \to 0$ as $\delta \to 0$. That means that $\nu(R) \to 0$ uniformly in the segment $[1, R_1]$. The fact that R_1 itself tends to infinity results simply from our assumption $M = \infty$ and is not important here (so does R_2 although extremely slowly). We know from eqs.(28, 29) that $R, R_1 < M^{3/4}$ for all $\nu > 0$ and $R \to M^{3/4}$ as $\nu \to \infty$, Figure 3a. Coming back to the $\delta \to 0$ limit we see that the function $\nu(R, \delta) \to \nu_0(R)$. Furthermore, $\nu_0(R) \equiv 0$ for $R \in [1, R_1]$ and rises sharply at some $R_0 \in [R_1, M^{3/4})$. That means that if we now let the actual injection rate tend to zero from above, R will tend to $R_0 \geq R_1$ instead of $R = 1$ as is always the case in kinetic description for all $\delta > 0$. As we have seen R_0 may be rather large whereas in the TFM $R_0 = 7$ which is only because of the complete subshock smoothing. Thus, there is nothing surprising that $R \to R_0 \neq 1$ as $\nu \to 0$ in the two-fluid description. From the viewpoint of the superior kinetic solution this transition reads $\delta \to 0$, $\nu \to 0$ and yields $R \to R_0(M) \gg 1$ for $M \gg 1$. The fact that R_0 turns out to be equal 7 in the TFM is not important in the present context, as we mentioned. On inverting the sequence, i.e. letting $\nu \to 0$, $\delta \to 0$ we clearly get $R \to 1$, but this is definitely beyond the TFM since the transition $\delta \to 0$ has already been made during the derivation of the two-fluid equations. The sensitivity to the order of the limit transitions is a signature of the singular dependence of the kinetic solution upon δ at $\delta = 0$ and has, at least formally, nothing to do with the TFM.

For $M < \infty$ the above consideration needs some modification with an involved algebra but the main conclusion remains: since in the limit process $\delta \to 0$, $\nu_2 > \nu_1$ for sufficiently large M, a correct behavior of $R(\nu)$ at vanishing ν, i.e. the transition $R \to 1$ as $\nu \to 0$ is impossible within the TFM.

Let us look now into the issue of the subshock smoothing. It was shown in paper I that the subshock may indeed be reduced significantly and its strength for sufficiently large M depends on only one parameter. This is a most important system parameter governing the nonlinear shock acceleration. It equals

$$\Lambda \equiv \frac{\Lambda_1}{M^{3/4}} \equiv \frac{\nu}{\delta \cdot M^{3/4}} \tag{38}$$

The subshock strength, when it is weak, scales as (see eq.(83) in paper I)

$$r_{\rm s} - 1 \sim 1/\Lambda, \quad \Lambda \gg 1 \tag{39}$$

Since the TFM implies that $\delta = 0$, there is again nothing strange that it produces a completely smooth solution $r_{\rm s} = 1$.

Therefore the TFM solution is completely understandable and in certain respects may serve as a limit of the full kinetic solution. The problem is that it is a singular limit and it

might thus formally be applied – provided that the closure parameters are found – only in a small (in fact measure zero) part of parameter space, namely where $\Lambda^{-1} \equiv \delta \cdot M^{3/4}/\nu = 0$. The kinetic solution differs dramatically from the TFM solution even for $1 \ll \Lambda < \infty$. This is perhaps the price we have to pay for describing an intrinsically kinetic problem quasi hydrodynamically.

Turning now to the situation of finite Λ, i.e., $p_1 < \infty$ which, as we just have seen, should be addressed kinetically, we note that the parameter p_1 may vary not only from one steadily accelerating shock to another but it can grow as a maximum momentum in a time dependent acceleration process and can thus pass through the critical values of the corresponding bifurcation diagram. If this time evolution is sufficiently slow the steady state solution with slowly varying parameters should be a good approximation provided that the temporal behavior of these parameters is determined. We continue our bifurcation analysis from this perspective in the next section.

5. Possible scenario of time dependent acceleration

It is convenient to argue in terms of a familiar projection method (see *e.g.,* Joseph 1976 for its hydrodynamic version). We start from a general evolution equation in a symbolic form that governs the acceleration process

$$\frac{dw}{dt} = W(w, \mu) \tag{40}$$

where w is a suitable vector of state of the system that contains both the particle distribution $g(x, p, t)$ and the flow structure $u(x, t)$. Eq.(40) implies the diffusion-convection equation along with the continuity and Navier-Stokes equations in appropriate representations. We denoted as μ the set of relevant parameters like M and ν. As one of the projections of w (or u) we may choose $R \equiv u_1/u_0$ and the correspondent component of eq.(40) takes the form of an ordinary differential equation (ODE)

$$\frac{dR}{dt} = W_1(R, r_{\rm s}, p_1, \ldots, \mu) \tag{41}$$

Here we regard p_1 as a dependent variable like R and $r_{\rm s}$ and others denoted by the ellipsis rather than a parameter that belongs to the set μ which would be appropriate for a problem with the fixed cut-off momentum considered in the previous sections. One may also write the similar equations for $r_{\rm s}$, p_1 etc.

$$\frac{dr_{\rm s}}{dt} = W_2(R, r_{\rm s}, p_1, \ldots, \mu) \tag{42}$$

$$\frac{dp_1}{dt} = W_3(R, r_{\rm s}, p_1, \ldots, \mu) \tag{43}$$

What we have described in the preceding sections corresponds to $W_3 \equiv 0$ as an external constraint and we have found in fact our steady state solutions as solutions of the system

$$W_1 = 0, \quad W_2 = 0 \tag{44}$$

The last equation being resolved for $r_{\rm s}$ simply yields the R-H relation (5), whereas the first equation was studied in Sec.3 and for a fixed ν it provides the solution $R = R(p_1, M)$, represented *e.g.,* in Figs.3-4. Now it is convenient to depict this solution for different values of ν and for a fixed M as shown in Figure 6. For $p > p_{1\,\rm cr}$ and depending on ν and p_1 either one or three solutions occur. Let us fix $\nu = c$ for which the three solutions coexist in the interval $p_1^{(1)} < p_1 < p_1^{(2)}$, whereas for $p_1 < p_1^{(1)}$ ($p_1 > p_1^{(2)}$) only the inefficient (efficient) solution occurs. It is obvious that the time scale in eq.(42) is much shorter than that in eqs.(41) and (43) since R and p_1 variations are followed by the subshock strength $r_{\rm s}$ almost instantaneously. The latter may be then found from the equation $W_2(R, r_{\rm s}, p_1) = 0$ as a function of R and p_1 and be then substituted into eqs.(41) and (43). The time scales in eqs.(41) and (43) are generally not well separated. Nevertheless, since significant variations in R can take place under constant p_1 (not vice versa, however), we may assume tentatively that p_1 evolves slowly compared to the transition time between equilibria of eq.(41) that are given by $W_1(R, r_{\rm s}(R), p_1) = 0$ and plotted schematically in Figure 6 as $R(p_1)$.

Relaxing the condition $W_3 = 0$ suggests the following scenario of the time dependent acceleration. Suppose $\nu = c = const$ and the cut-off momentum $p_1(t)$ increases in time beginning from a value that is in the interval $p_{1\,\rm cr} < p_1 < p_1^{(1)}(\nu)$ (Figure 6). As long as the lower branch $R_{\rm l}(p_1)$ is stable, the system will advance along this branch towards higher p_1. When the second critical point $p_1^{(2)}(\nu)$ is reached, the flow profile together with the underlying particle distribution will restructure in such a way that a much more efficient acceleration regime corresponding to the upper branch $R_{\rm u}(p_1)$ emerges. If $R_{\rm u}(p_1^{(2)}) < M^{3/4}$ the subshock will not be reduced significantly which is the necessary condition for keeping injection at the same level, and the acceleration process may continue towards even higher p_1 along the efficient branch $R_{\rm u}$. It is interesting to note that if, after this transition p_1 starts to decrease instead, there will be a hysteretic behavior in the acceleration process as it is shown in Figure 6. The decrease of p_1 may be caused by an enhance of losses due to *e.g.,* parameter variations on the shock path.

If $R_{\rm u}(p_1^{(2)}) > M^{3/4}$ the transition to the upper branch will be accompanied by a strong subshock reduction and, as a result, by a considerable variation in ν. It should be noted, however, that if the subshock is still not very weak, say $r_{\rm s} \gtrsim 2$, then ν not necessarily decreases with decreasing $r_{\rm s}$ (see Malkov & Völk 1995). This is mostly an effect of normalization of injection rate ν, the number of injected particles does decrease since the spectrum becomes steeper at $p \sim p_0$ (see eq.(15)). Besides that, this consideration is based on a purely kinematic treatment of the leakage from the downstream medium and, in addition, is limited to relatively strong subshocks. When $r_{\rm s}$ drops to $r_{\rm s} \gtrsim 1$ the injection rate ν may also become very low. This means that the solution must move to a lower level

$\nu = const$ to remain quasi-steady. Such a process will depend very much on the injection model in use and on the underlying subshock dissipation mechanism which are beyond the scope of the present paper (see Malkov 1997c, Malkov & Völk 1997). One may only hypothesize that if the subshock reduction is very strong and ν substantially decreases during this transition, the solution should either evolve being close to the critical injection rate ν_1 or, if ν drops essentially below ν_1 the solution may return to the lower branch again to display thus essentially time dependent behavior.

The above consideration implies the stability of the branch R_l so that the stability of $R_{\rm u}$ and instability of $R_{\rm i}$ follow just from the continuity of $W_1(R)$ in eq.(41). A different situation occurs when the branch $R_{\rm i}$ is stable, at least for certain values of p_1, and therefore R_l and $R_{\rm u}$ are both unstable for the same p_1. Then, as p_1 grows, the solution evolves along $R_{\rm i}$ up to the point $p_1 = p_1^{(2)}$, beyond which the acceleration process again cannot continue in a quasi steady manner. In a similar situation occurring in the TFM it is usually argued that the intermediate solution is unstable (DV). This is indeed typical for systems with S-type response curves like ours. We do not consider this question here in any detail but we note that an extended system of ODEs (eqs.(41, 42, 43)) or even its further extensions will almost certainly possess a much more rich invariant manifold than the fixed points R_l, $R_{\rm i}$ and $R_{\rm u}$ of eq.(41).

Interestingly, on the branches R_l and $R_{\rm u}$, R increases with M whereas it decreases with M on the branch $R_{\rm i}$ (see *e.g.,* Figure 4). Similarly, under fixed M and p_1, R_i decreases with ν, again opposite to R_l and $R_{\rm u}$ (Figures 2, 3b, 6). This region of an anomalous behavior (like negative differential conductivity) may even be identifiable in steady state numerical simulations. It should be noted, however, that for very large Mach numbers $M > R^{4/3}$ the compression ratio becomes practically independent of M on the all three branches (see also paper I).

6. Discussion and conclusions

The early works on the nonlinearly modified CR shocks inspired the hope that, because of a very high acceleration efficiency in the nonlinear regime, the overall CR production should not be very sensitive to injection and just a qualitative understanding of this complicated process suffices for quantitative calculations of acceleration efficiency. The CR dominated (efficient) solutions of the two-fluid model (DV) strongly supported this idea. In fact, such an optimism rests on the limited amount of energy available in the gas flow to be converted into CRs. Indeed, if we consider a strong shock ($M \gg 1$) we may calculate the acceleration efficiency, or the coefficient of the flow energy conversion, as $\varepsilon_{\rm conv} = P_{\rm c}(0)/\rho_1 u_1^2 = 1 - 1/R$, eq.(3). Whenever the acceleration process is known to be in the nonlinear regime ($R \gg 1$), almost all the flow energy goes into CRs, practically independent of anything at all.

The main issue now is, under which circumstances the system may indeed be in a highly nonlinear acceleration regime. As we have seen, the answer to *this* question depends *critically* on the injection rate: infinitesimal variations of ν in the vicinity of ν_1 or ν_2 can result in finite (and typically very large) variations of R due to transitions between different branches. Also solutions belonging to the same branch are typically very sensitive to the injection rate ν. This may be easily understood from the inspection of *e.g.,* Figure 2 and Figure 3a where only on the inefficient branch R varies relatively slowly with ν, while in the cases of intermediate and especially efficient solution R changes very rapidly with injection. There is of course an injection insensitive region belonging to efficient solution where the compression $R(\nu)$ approaches its upper bound $R \sim M^{3/4}$ at given M (see Figure 3a, where this region may be identified as a very sharp growth of the function $\nu(R, M)$ in the farthermost corner of the plot). Such a behavior is caused by the requirement of a finite subshock. It should be noted that this scaling has indeed been observed in some numerical works with fixed injection rates (*e.g.,* Berezhko, Ksenofontov & Yelshin 1995). However, this situation occurs at sufficiently large values of ν and diminished $r_{\rm s}$ and it is doubtful that such a high injection rate is possible at a weak subshock. For smaller ν, when $\nu \ll \delta \cdot M^{3/4}$ (the system parameter $\Lambda \ll 1$) an important signature of the stationary acceleration is that the compression ratio is practically independent of M (see paper I for further details).

Physically, the injection rate should be calculated selfconsistently using the solution of injection problem given subshock parameters. The solution of this problem provides a function $\nu = \nu_{\rm s}(R, M)$. Then isolated solutions for $R = R(M)$ might be obtained as intersection points of the curves $\nu_{\rm s}$ and ν (as shown in Figure 1). This solution may or may not be multiple depending on the character of the function $\nu_{\rm s}$. In any case, the bifurcation diagrams alone do not suffice for determining the actual acceleration efficiency. The calculation of the injection $\nu_{\rm s}$ as a function of shock characteristics is equally important for this purpose. It should also be born in mind that the model considered here and in paper I gives an upper bounds to the actual acceleration efficiency. A number of not included factors may significantly decrease compression ratio R, acceleration efficiency and the spectrum hardness (see paper I for a relevant discussion).

Turning to the time dependent acceleration we note that unless the scenario suggested in the previous section is totally unrealistic, a critical quantity that would determine the CR production is the cut-off momentum $p_1^{(2)}$ beyond which the system jumps to the efficient acceleration regime. According to eq.(37) $p_1^{(2)} \propto \exp(1/\nu)$. Since in the Bohm limit we may write $p_1(t) \propto t$, the corresponding critical time $t_{\rm crit} \propto \exp(1/\nu)$. In an accelerating object of a finite life time τ (*e.g.,* supernova remnant, SNR) the main question, of course, is whether the condition $\tau > t_{\rm crit}$ is fulfilled. This is again extremely sensitive to the injection rate.

Theoretically, the injection rate $\nu_{\rm s}$ must not necessarily be as high as ν_2 for the acceleration process to become efficient. The condition $\nu_{\rm s} > \nu_1$ could suffice provided that the lower branch R_l (Figure 6) looses stability for $p_1 \lesssim p_1^{(1)}$. Since for large values of p_1,

$\nu_2 \gtrsim 10\nu_1$ (see Figure 5), this may determine the outcome of the acceleration process completely. Another possibility to overcome the high ν_2 threshold is an essentially stronger time dependence of the acceleration process than that discussed in the preceding section. Basically, the bifurcation picture of this system is quite rich and promises an interesting dynamics. This is the more so as governing parameters are themselves subject for a temporal evolution. They may change significantly during the acceleration process in a variety of astrophysical environments. These variations may be of a quasi-external type like *e.g.,* decrease of the Mach number when the shock slows down. Equally important may be an intrinsic variability associated with the growth of the maximum energy or with the heating of the upstream plasma by the CR driven turbulence (Völk, Drury, & McKenzie 1984). Therefore, to comprehend the acceleration dynamics we must face the injection problem together with the physics of subshock dissipation and treat these problems selfconsistently with the above bifurcation analysis. The fact that this system displays very much hysteresis emphasizes the necessity of this approach.

It is important to recognize that there is a serious drawback in the way to a full calculation of the acceleration efficiency in concrete astrophysical shocks, like *e.g.,* SNR shocks. It originates from the threshold nature of the acceleration process. Indeed, the flow structure changes quasi-abruptly when the critical injection ν_2 drops below $\nu_{\rm s}(R_2)$ as p_1 grows (or $\nu_{\rm s}(R_1)$ becomes smaller than ν_1). Since the function $\nu_{\rm s}$ is very sensitive to local subshock conditions (a local orientation of the magnetic field is perhaps the most obvious and very important factor here), this transition occurs first at those parts of the shock surface where $\nu_{\rm s}$ reaches its maximum. This must result in 'hot spots' or 'discharge' zones in the shock front where the acceleration becomes efficient. Then, the flow structure will be essentially 3-dimensional (or at least quasi 2-dimensional), quite complicated and probably unsteady. The inhomogeneity of the ambient medium (see *e.g.,* McKee 1982) may very well result in a similar effect. Clearly, the one-dimensional calculations, even with a properly determined injection rate $\nu_{\rm s}(R, M)$ may give at best an upper bound to the acceleration efficiency. Even if the flow remains quasi-laminar the overall efficiency will be reduced according to the surface density of the hot spots on the shock front. Besides that the losses from the hot spots into the neighboring regions of inefficient acceleration may significantly reduce the maximum energy. A very important consequence of this would be the corresponding increase of the critical injection, eq. (36) which may drive the system below the threshold of the efficient acceleration.

I would like to thank Heinz Völk for intersting discussion. This work was done within the Sonderforschungsbereich 328, "Entwicklung von Galaxien" of the Deutsche Forschungsgemeinschaft (DFG).

REFERENCES

Achterberg, A., Blandford, R. D., & Periwal, V. 1984, A&A, 132, 97

Axford, W. I., Leer, E., & Skadron, G. 1977, Proc. 15th ICRC (Plovdiv) 11, 132

Bell, A. R. 1978, MNRAS, 182, 147

Blandford, R. D., & Ostriker, J. P. 1978, ApJ, 221, L29

Blandford R.D., Eichler D., 1987, Phys. Rept., 154, 1

Berezhko, E. G., Ksenofontov, L., & Yelshin 1995, Nucl. Phys. B (Proc. Suppl), 39A, 171

Drury, L. O'C. 1983, Rep. Prog. Phys. 1983, 46, 973

Drury, L. O'C., & Völk, H. J. 1981, ApJ, 248, 344 (DV)

Drury, L.O'C., Markiewicz, W.J., Völk, H.J. 1989, A&A, 225, 179

Drury, L. O'C., Völk, H. J. & Berezhko, E. G. 1995, 299, 222

Falle, S. A. E. G. & Giddings, J. R. 1987, MNRAS, 225, 399

Gleeson, L. J., & Axford, W. I. 1967, ApJ, 149, L115

Jones F. C., Ellison D. C., 1991, Space Sci. Rev. 58, 259

Joseph, D. D., Stability of Fluid Motion I, Springer Tracts in Natural Philosophy , Vol. 27, Springer, Berlin, Heidelberg, New York 1976

Kang, H., & Jones, T. W. 1990, ApJ, 353, 149

Krimsky, G.F., 1977, Dokl. Akad. Nauk SSSR 234, 1306 (Engl. Transl. Sov. Phys.-Dokl. 23, 327).

Malkov, M. A. 1997a, to appear in ApJ, vol.485 (paper I, astro-ph/9707152)

Malkov, M. A., 1997b, submitted to Phys. Rev. Lett.

Malkov, M. A., 1997c, submitted to Phys. Rev. E

Malkov, M. A., & Völk, H. J. 1995, A&A, 300, 605

Malkov, M. A., & Völk, H. J. 1996, ApJ, 473, 347 (MV96)

Malkov, M. A., & Völk, H. J. 1997, to appear in Adv. Space Res.

McKee, C. F. 1982, in Supernovae: A Survey of Current Research, ed. M. J. Rees & R. J. Sroneham, 433

Parker, E. N. 1965, Planet. Space Sci., 13, 9

Ptuskin, V. S. 1981, Ap&SS, 76, 265

Völk, H. J., Drury, L O'C, & McKenzie, J.F. 1984, A&A, 130, 19

Fig. 1.— The nonlinear response R of an accelerating shock to the thermal injection ν represented in the form of a single valued function $\nu(R)$. Given $\nu \in (\nu_1, \nu_2)$ there are three substantially different acceleration regimes. A few possible graphs of $\nu_{\rm s}(R)$ (see Sec.6) are also drawn with the thin lines.

Fig. 2.— a.) Response curves calculated from eq.(29) (branches 2-3, dashed line) and from eq.(35) (branches 1-2, solid line), for $M = \infty$ and $\delta = 10^{-4}$. b.) Blow up of the peak in Figure 2a.

Fig. 3.— a.) The surface of stationary solutions $\nu(R, M)$ plotted for $\delta = 10^{-3}$. b.) The same as in Figure 3a but ν is given as a function of R and δ for $M = \infty$. Both surfaces are trimmed at high ν.

Fig. 4.— The same as in Figure 3a but this time in the form of the contourplot $\nu = const$ and for smaller M, not shown in Figure 3a.

Fig. 5.— Critical injections ν_1 and ν_2 versus δ given by eqs.(36) and (37).

Fig. 6.— Curves of constant ν drawn schematically on the basis of the surface plot shown in Figure 3b. The bifurcation of acceleration occurs when ν crosses its critical value, $\nu_{\rm cr}$ (the solid curve marked by $\nu = \nu_{\rm cr}$). For $\nu < \nu_{\rm cr}$ and $p_1 > p_{1\,{\rm cr}}$ three different acceleration regimes emerge for p_1 being within a certain interval (the solid curve marked by $\nu = \nu_{\rm c}$). These regimes, R_l, R_i, $R_{\rm u}(p_1)$ correspond to the 1,2,3 branches in Figure 1. The two remaining light curves correspond to ν- values $c < \nu < \nu_{\rm cr}$ and $\nu < c$.

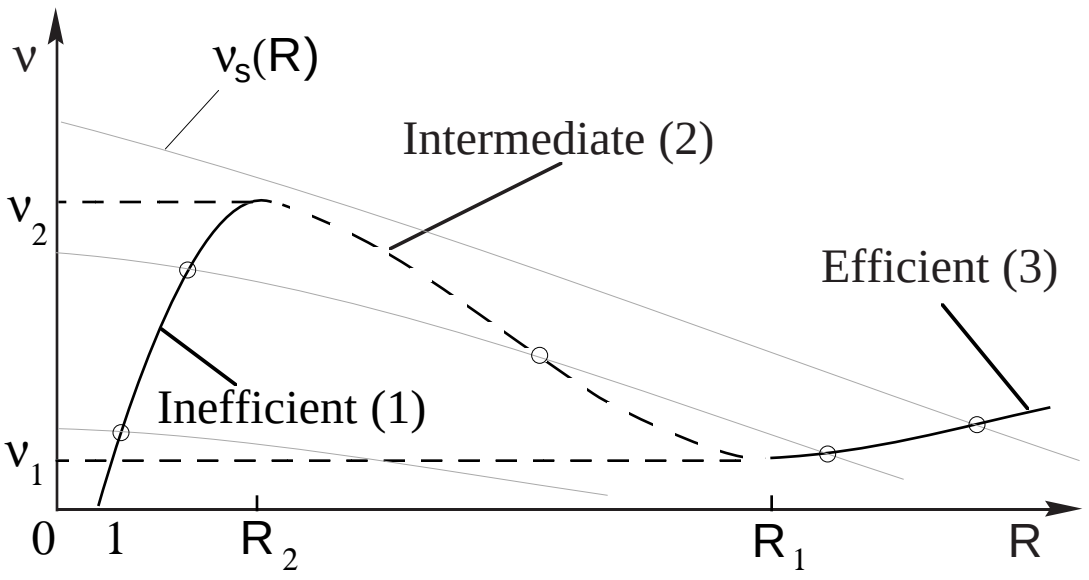
ν
$\nu_s(R)$
Intermediate (2)
ν_2
Efficient (3)
Inefficient (1)
ν_1
0
1
R_2
R_1
R

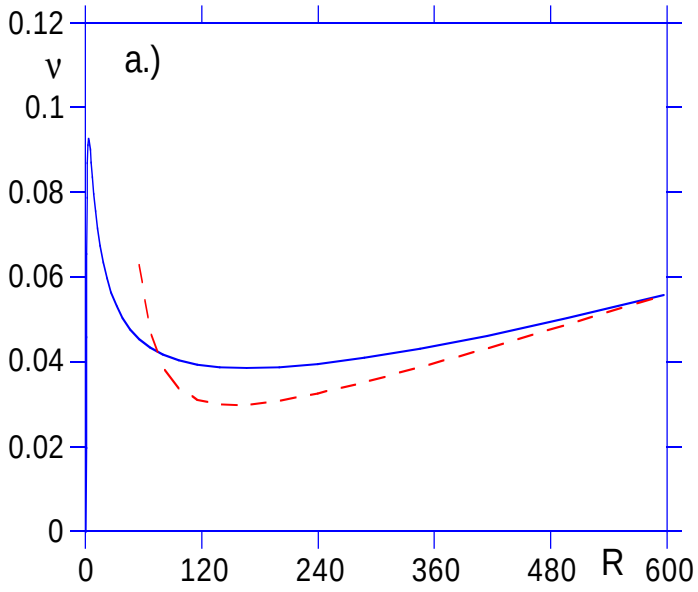
0.12
ν
a.)
0.1
0.08
0.06
0.04
0.02
0
0
120
240
360
480
R
600

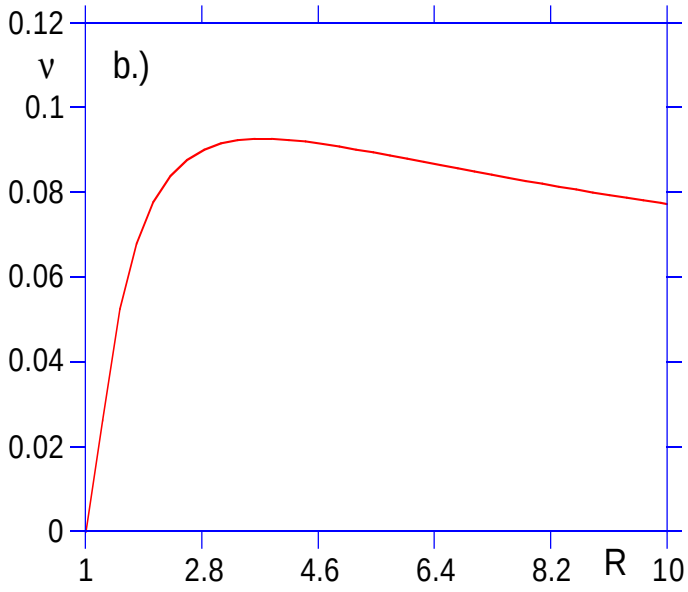
0.12
ν
b.)
0.1
0.08
0.06
0.04
0.02
0
1
2.8
4.6
6.4
8.2
R
10

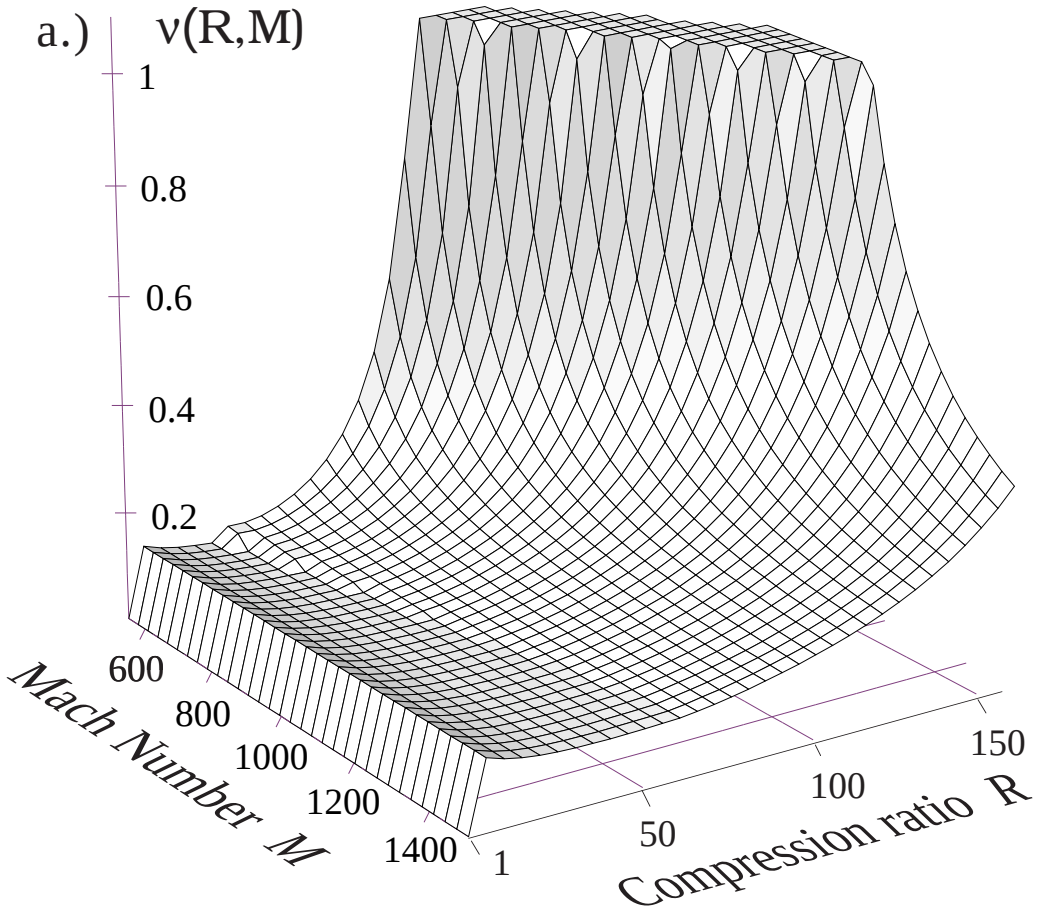
a.)
ν(R,M)
1
0.8
0.6
0.4
0.2
600
800
1000
1200
1400
Mach Number M
1
50
100
150
Compression ratio R

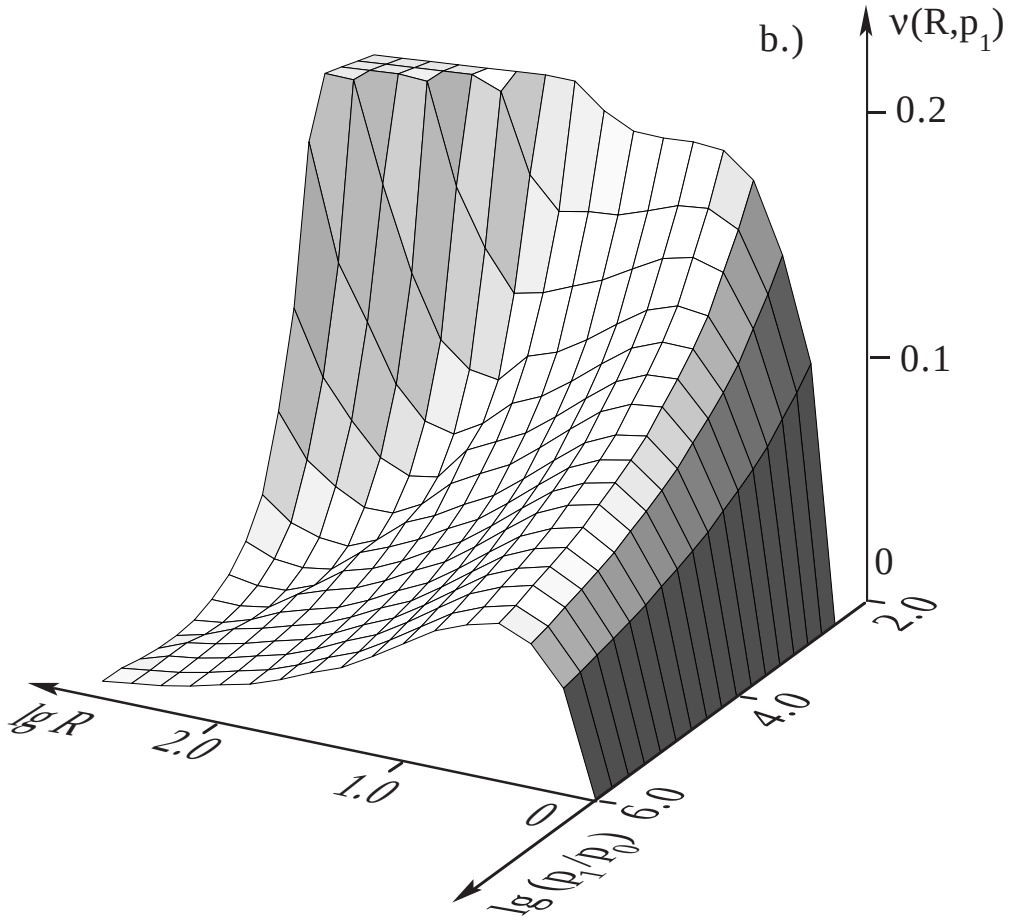
b.)
ν(R,p1)
0.2
0.1
0
2.0
4.0
6.0
lg(p1/p0)
0
1.0
2.0
lg R

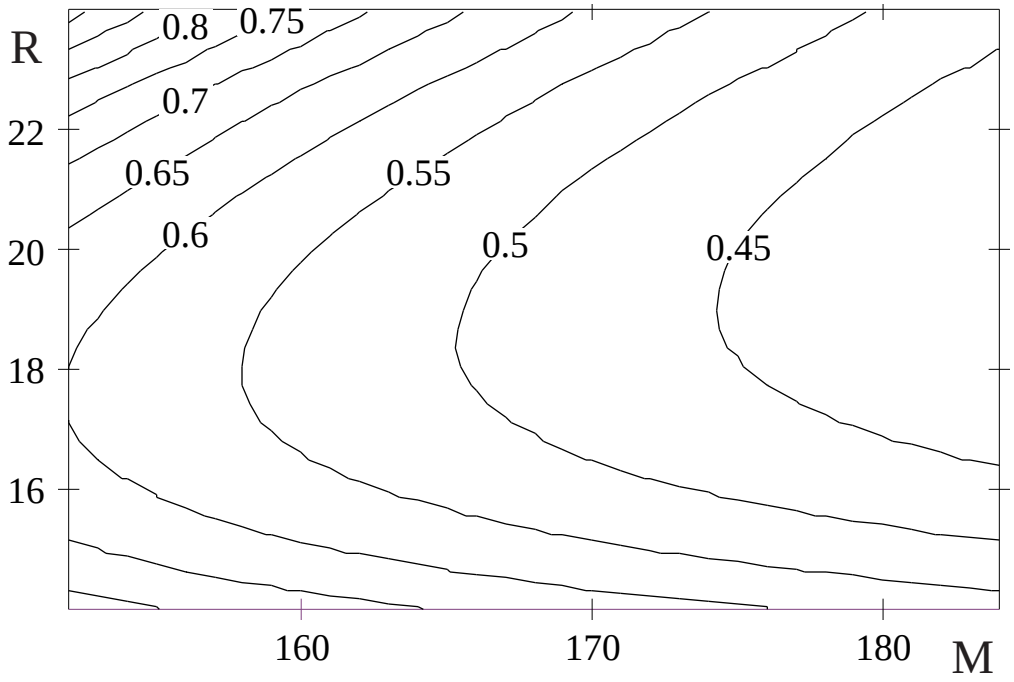
R
22
20
18
16
0.8
0.75
0.7
0.65
0.6
0.55
0.5
0.45
160
170
180
M

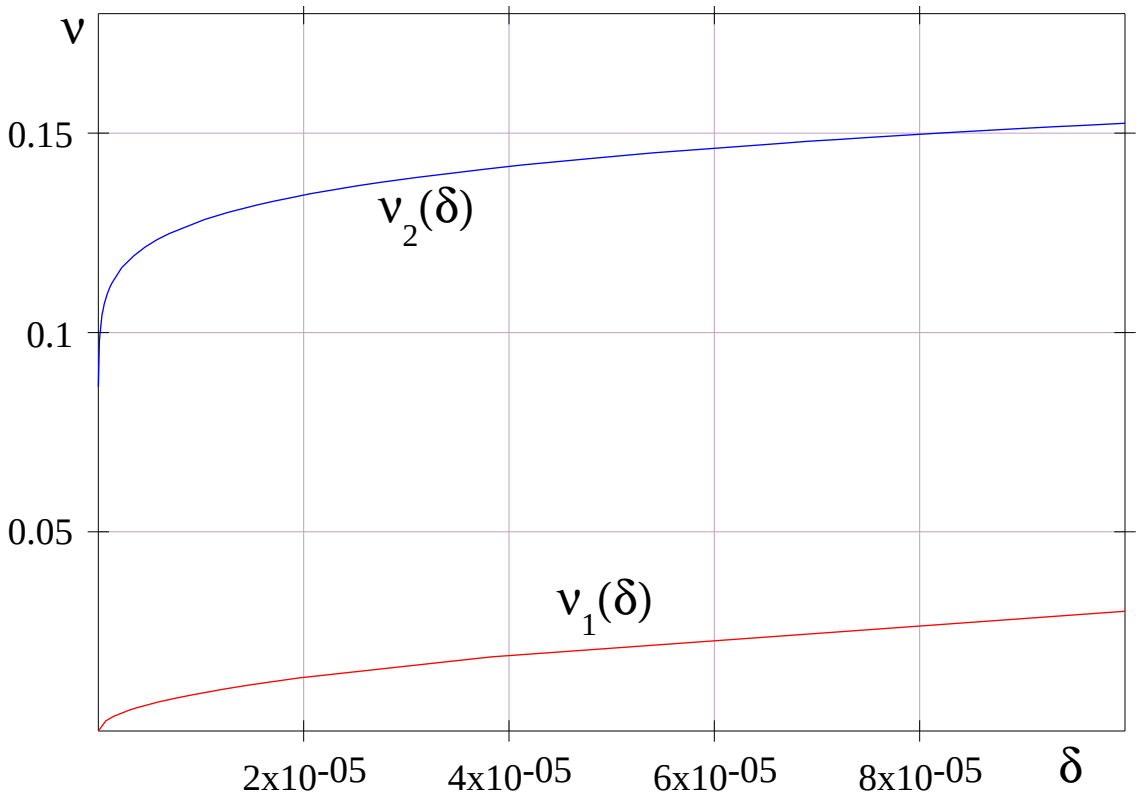
ν
0.15
0.1
0.05
ν2(δ)
ν1(δ)
2x10-05
4x10-05
6x10-05
8x10-05
δ

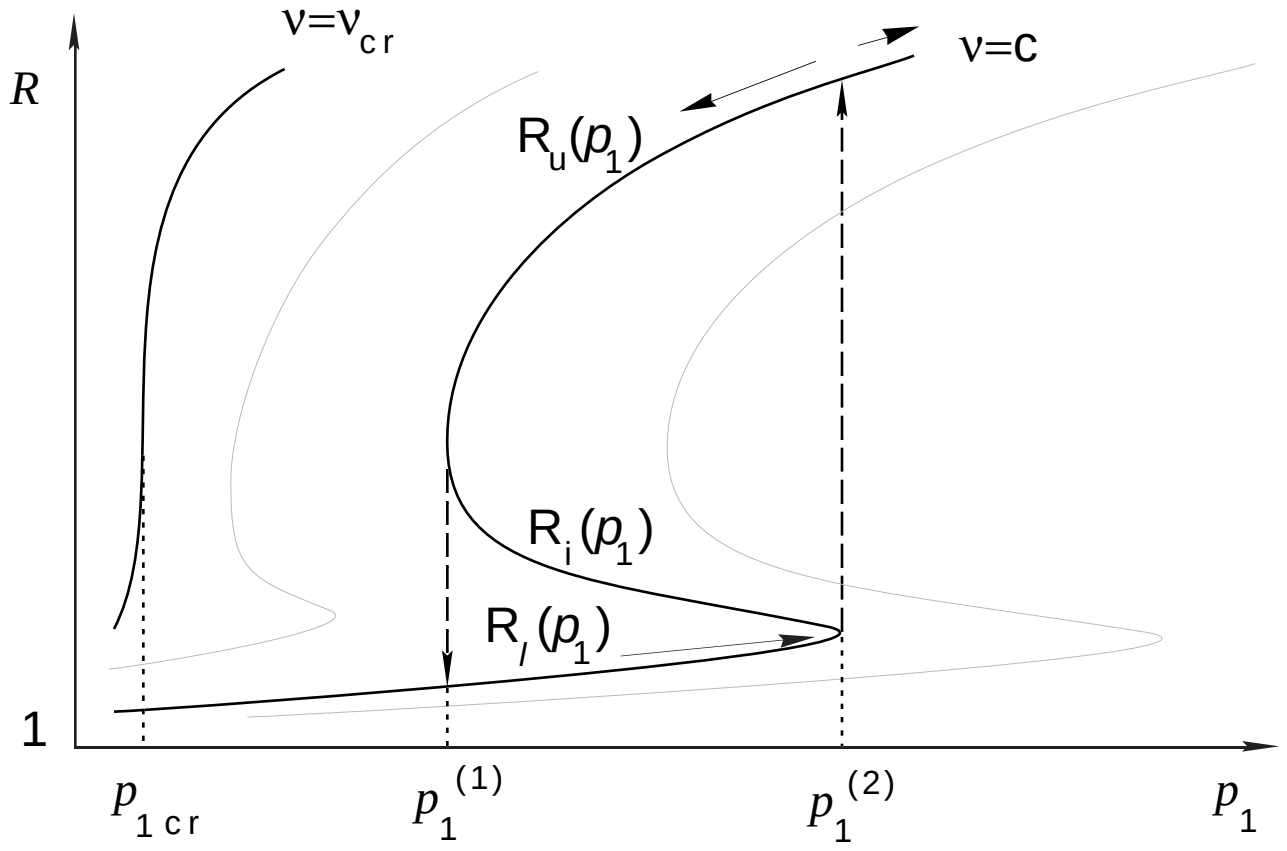
ν=ν cr
ν=c
R
R u (p 1)
R i (p 1)
R l (p 1)
1
p 1 cr
p 1 (1)
p 1 (2)
p 1